Supplemental Material

Supplemental figure legends

Figure S1. The biogenesis and transport of SV precursors are normal in *fat-3* mutants. (A) The endogeneous level of synaptobrevin (SNB-1) in *fat-3(wa22)* mutants is similar to that of WT animals. Western blots for SNB-1 and UNC-64-syntaxin (SYX; control) of membrane protein extracts (45 μg) from WT, *fat-3(wa22)*, *unc-57(ok310)-endophilin* and *snb-1(md247)* animals. (B) SNB-1::GFP total fluorescence (% of WT) in neurons. Total fluorescence is defined as the mean of the fluorescence measurements made from the GABAergic neuronal cell bodies DD1, VD1 and VD2, and from GABAergic synapses in the dorsal nerve cord. (C and D) Electron micrographs of neuronal cell bodies from a WT (C) and a *fat-3(lg8101)* mutant (D). Vesicles of 30 to 50 nm (arrowheads) were present in both strains in similar amounts. N: nucleus. Scale bar: 1 μm. (E) Density of 30-50 nm vesicles in neuronal cell bodies. Thin section images of well-fixed neurons were analyzed for 103 neuronal cell bodies from six WT animals and 68 neuronal cell bodies from four *fat-3(lg8101)* mutants. (F-H) Animals defective in the transport of precursor vesicles, such as *unc-104-kinesin* mutants (Zhao and Nonet, 2001; Klopfenstein and Vale, 2004), accumulate high levels of SV components, including GFP-tagged ones, in their neuronal cell bodies. We therefore looked at the number of neuronal bodies showing detectable SNB-1::GFP fluorescence and quantified this fluorescence. (F) Confocal images of the three specific GABAergic neuronal cell bodies DD1, VD1 and VD2 we selected to perform quantitative analysis. We chose these cell bodies because they were clearly visible and because their fluorescence in WT animals was often minimal, making it easier to detect changes. Scale bar: 10 μm. (G) Average number of neuronal cell bodies (DD1, VD1 and VD2) per animal showing detectable SNB-1::GFP fluorescence. We found that this number was similar in WT animals and *fat-3(wa22)* mutants (2.14 ± 0.14 versus 2.16 ± 0.16). (H) Intensity of SNB-1::GFP fluorescence (F/F0) within the neuronal cell bodies DD1, VD1

and VD2. This intensity was not significantly different between WT animals and *fat-3(wa22)* mutants (6.95 ± 0.39 versus 8.59 ± 0.76; P = 0.09) and was similar to that observed in the endocytosis mutant *unc-57(ok310)-endophilin* (8.11 ± 0.65, *n* = 16; not shown), which is defective in SV recycling but not in precursor vesicle transport (Schuske *et al.*, 2003). F is the measured fluorescence and F0 is the fluorescence background. (I) SNB-1::GFP fluorescence (% of WT) at sites of release in the dorsal nerve cord (Dnc) was not statistically different between *fat-3(wa22)* mutants and WT animals (111 ± 4.7% versus 100 ± 4.8%; P = 0.10), suggesting that normal amounts of SV precursors reach release sites in *fat-3(wa22)* mutants. The quantification was performed on a 50 µm portion 28 µm posterior to the ring motor neuron RMED (schematic in figure 1 A). In (B), (E), (G), (H), and (I) data were plotted as mean ± SEM.

Figure S2. Synaptobrevin is partially mislocalized in *fat-3* mutants. (A) Average SNB-1::GFP fluorescence intensity in the axonal plasma membrane between synapses (Fa) and in the puncta (Fp). Fa (left graph) was significantly increased in *fat-3(wa22)* mutants (39.04 ± 2.93) and in *unc-57(ok310)-endophilin* mutants (67.28 ± 6.38) compared to WT animals (21.44 ± 1.47). Fp (right graph) was similar in all strains tested (WT, 221.02 ± 5.66; *fat-3(wa22)*, 224.64 ± 3.03; *unc-57(ok310)-endophilin*, 225.64 ± 2.37). Fa and Fp are expressed as average grey value. Resolution: 1 pixel = 400 nm. Data are plotted as mean ± SEM. ***, P < 0.0005. (B) Distribution and quantification of SNB-1::GFP mislocalization at high resolution (1 pixel = 130 nm). SNB-1::GFP was partially mislocalized in *fat-3(wa22)* and *unc-57(ok310)-endophilin* mutants, when compared to WT animals. Fa (left graph) was 56% higher in *fat-3(wa22)* mutants (35.53 ± 4.23; P = 0.048) and 131% higher in *unc-57(ok310)-endophilin* mutants (52.64 ± 10.12; P = 0.0041), compared to WT animals (22.76 ± 4.08). Fp (middle graph) was not significantly different in the three strains (WT: 125 ± 11.95; *fat-3(wa22)* mutants: 148.59 ± 9.35; *unc-57(ok310)-endophilin* mutants: 111.74 ± 16.46). Fa and Fp are expressed as average grey values. The diffusion values (right graph; see Materials and Methods for details on how diffusion was calculated) in *fat-3(wa22)* mutants (0.242 ±

0.026) and in *unc-57(ok310)-endophilin* mutants (0.467 ± 0.031) were 1.4-fold (P = 0.038) and 2.7-fold (P < 0.0001) greater than those in WT animals (0.172 ± 0.019), respectively. **, P < 0.05; ***, P < 0.005. (C) Distribution of the SV proteins RAB-3, SNT-1, UNC-11 and of endogenous SNB-1. The distribution of these proteins was followed by immunostaining. Confocal micrographs were taken at a resolution of 400 nm per pixel for RAB-3 and SNT-1 and of 130 nm per pixel for UNC-11 and endogenous SNB-1. In WT animals, all of these proteins were distributed in puncta, corresponding to clusters of SVs at neuromuscular junctions. RAB-3, SNT-1 and UNC-11 had a similar distribution in the *unc-57(ok310)-endophilin* mutant, suggesting that their localization is not affected by defects in SV recycling. Endogenous SNB-1 appeared partially mislocalized in the *fat-3(wa22)* mutant. We could only detect minimal changes of Fa in the *unc-57(ok310)-endophilin* mutant (not shown). The schematics show the portion of the nerve cord imaged for the indicated proteins as a black box. (D) Quantification of endogenous SNB-1 diffusion. The diffusion value of the *fat-3(wa22)* mutant (0.484 ± 0.03) was 1.26-fold that observed in WT animals (0.383 ± 0.02, P = 0.024) and was similar to that of the *unc-57(ok310)-endophilin* mutant (0.496 ± 0.032, n = 6, P = 0.79). The lower diffusion detected for endogenous SNB-1, particularly in *unc-57-endophilin* mutants in comparison to that observed for SNB-1::GFP, could be due to the lower sensitivity of detection by immmunofluorescence. Data are plotted as mean ± SEM. **, P < 0.05. Scale bars: 10 μm.

Figure S3. *fat-3* acts in the same genetic pathway as *synaptojanin* to retrieve synaptobrevin from the plasma membrane. (A) Average fluorescence intensity of SNB-1::GFP in the axonal plasma membrane between synapses (Fa). Fa values are normalized to WT values. Fa was significantly increased in *unc-57(ok310)-endophilin; fat-3(wa22)* double mutants (3.48 ± 0.49), when compared to *unc-57(ok310)-endophilin* (2.33 ± 0.245; P = 0.037) and *fat-3(wa22)* (1.64 ± 0.17; P = 0.0042) single mutants, suggesting that *fat-3* and *unc-57* act in parallel genetic pathways to promote SNB-1::GFP retrieval from the plasma membrane. The difference in Fa values obtained for *fat-*

3(wa22)unc-26(s1710)-synaptojanin double mutants (3.18 ± 0.39) and *unc-26(s1710)-synaptojanin* single mutants (2.51 ± 0.45) was not statistically significant (P = 0.27), suggesting that *fat-3* and *unc-26* operate in the same genetic pathway. Fa value for WT was: 1.00 ± 0.13. Data are plotted as mean ± SEM. **, P < 0.04; ***, P < 0.007. (B) Average fluorescence intensity of SNB-1::GFP in the puncta (Fp). Fp values are normalized to WT values. WT, 1.00 ± 0.08; *unc-57(ok310)-endophilin* mutants, 1.00 ± 0.09; *unc-26(s1710)-synaptojanin* mutants, 0.97 ± 0.12; *fat-3(wa22)* mutants, 1.30 ± 0.12; *unc-57(ok310)-endophilin; fat-3(wa22)* double mutants, 1.22 ± 0.19; *fat-3(wa22)unc-26(s1710)-synaptojanin* double mutants, 1.34 ± 0.21. Data are plotted as mean ± SEM.

Figure S4. The total levels of PtdIns(4,5)P_2 decrease in *fat-3* mutants. We measured PtdIns(4,5)P_2 levels in the total lipidic fraction extracted from WT, *fat-3(wa22)* mutant and *unc-26(s1710)-synaptojanin* mutant worms grown in the presence of 10 µCi/ml of tritiated inositol, allowing the labelling of PtdIns(4,5)P_2. (A) Partisphere SAX HPLC separation of deacylated lipid extracted from WT animals and *fat-3(wa22)* mutants. Relative migration of AMP, ADP, ATP and genuine deacylated PI(4,5)P_2 are indicated. (B) Levels of PtdIns(4,5)P_2 expressed as a percentage of the total lipid fraction extracted from mixed-stage populations of WT, *fat-3(wa22)* mutant and *unc-26(s1710)-synaptojanin* mutant whole-worms. We found a decrease of 27% in *fat-3(wa22)* mutants (4.40% ± 0.69%, *n* = 3) and of 20% in *unc-26(s1710)-synaptojanin* mutants (4.78% ± 0.44%, *n* = 3), compared to WT animals (6.03% ± 0.22%, *n* = 3). This decrease may reflect an adaptive response to decreased synaptojanin activity.

Supplemental References

Klopfenstein, D.R., and Vale, R.D. (2004). The lipid binding pleckstrin homology domain in UNC-104 kinesin is necessary for synaptic vesicle transport in *Caenorhabditis elegans*. Mol Biol Cell *15*, 3729-3739.

Schuske, K.R., Richmond, J.E., Matthies, D.S., Davis, W.S., Runz, S., Rube, D.A., van der Bliek, A.M., and Jorgensen, E.M. (2003). Endophilin is required for synaptic vesicle endocytosis by localizing synaptojanin. Neuron *40*, 749-762.

Zhao, H., and Nonet, M.L. (2001). A conserved mechanism of synaptogyrin localization. Mol Biol Cell *12*, 2275-2289.

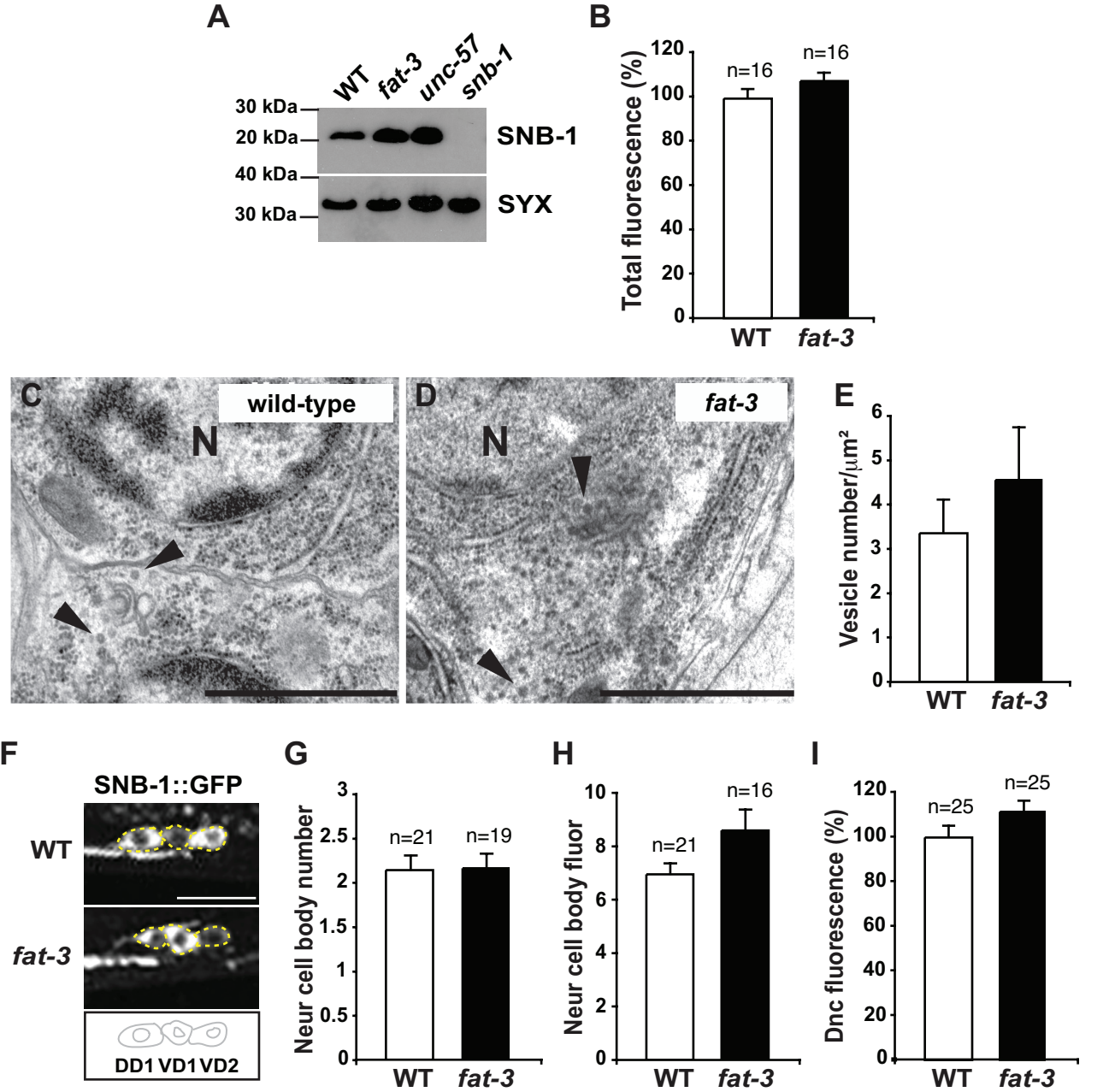
A
WT
fat-3
unc-57
snb-1
30 kDa
20 kDa
40 kDa
30 kDa
SNB-1
SYX
B
Total fluorescence (%)
120
100
80
60
40
20
0
n=16
n=16
WT
fat-3
C
wild-type
N
D
fat-3
N
E
Vesicle number/μm²
6
5
4
3
2
1
0
WT
fat-3
F
SNB-1::GFP
WT
fat-3
DD1 VD1 VD2
G
Neur cell body number
3
2.5
2
1.5
1
0.5
0
n=21
n=19
WT
fat-3
H
Neur cell body fluor
10
8
6
4
2
0
n=21
n=16
WT
fat-3
I
Dnc fluorescence (%)
120
100
80
60
40
20
0
n=25
n=25
WT
fat-3

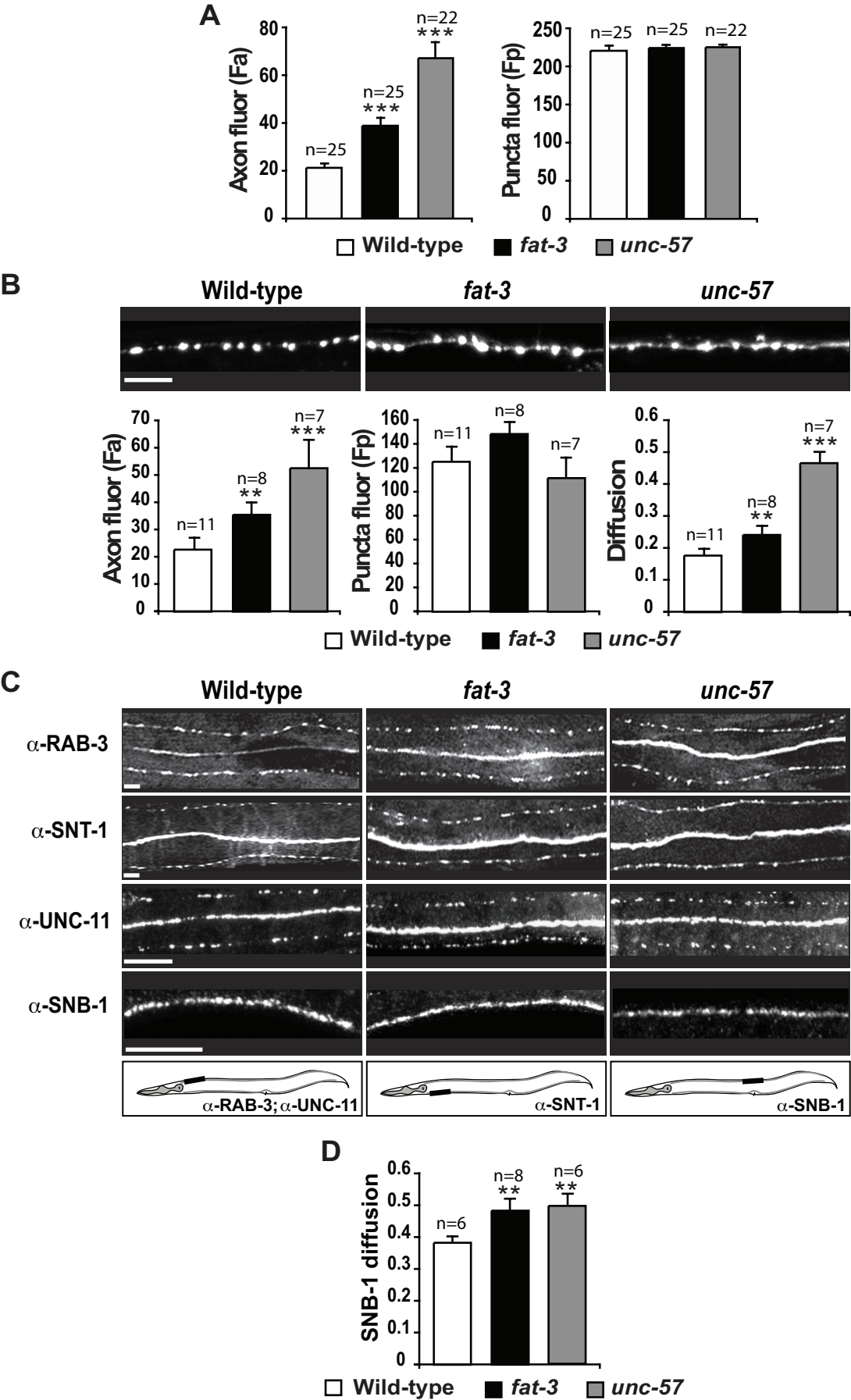
A
Axon fluor (Fa)
80
60
40
20
0
n=25
n=25
***
n=22
***
Puncta fluor (Fp)
250
200
150
100
50
0
n=25
n=25
n=22
Wild-type
fat-3
unc-57
B
Wild-type
fat-3
unc-57
Axon fluor (Fa)
70
60
50
40
30
20
10
0
n=11
n=8
**
n=7
***
Puncta fluor (Fp)
160
140
120
100
80
60
40
20
0
n=11
n=8
n=7
Diffusion
0.6
0.5
0.4
0.3
0.2
0.1
0
n=11
n=8
**
n=7
***
Wild-type
fat-3
unc-57
C
Wild-type
fat-3
unc-57
α-RAB-3
α-SNT-1
α-UNC-11
α-SNB-1
α-RAB-3;α-UNC-11
α-SNT-1
α-SNB-1
D
SNB-1 diffusion
0.6
0.5
0.4
0.3
0.2
0.1
0
n=6
n=8
**
n=6
**
Wild-type
fat-3
unc-57

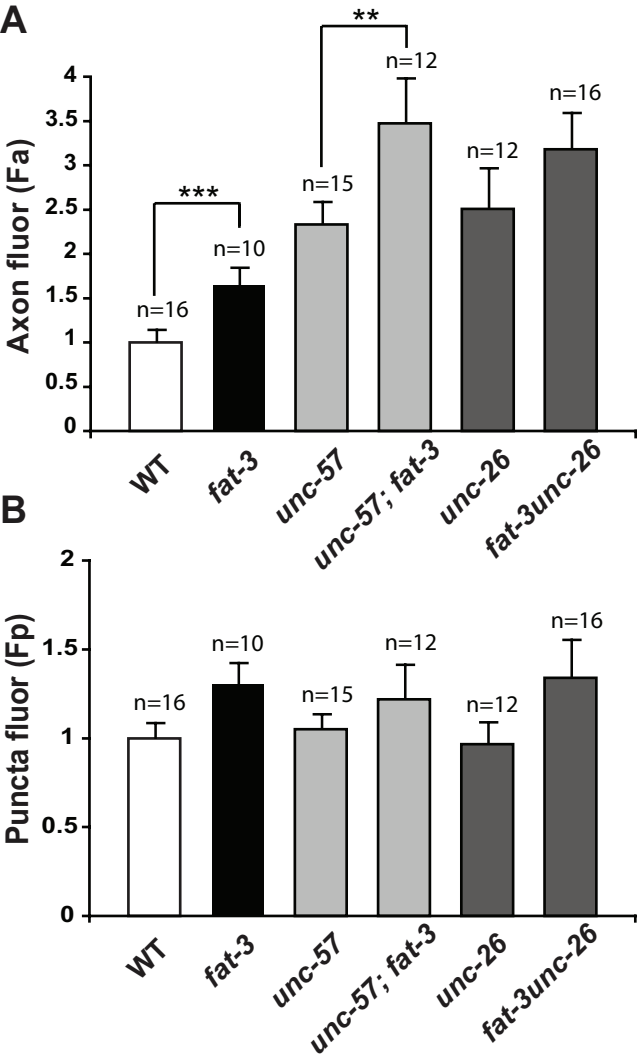
A
Axon fluor (Fa)
4
3.5
3
2.5
2
1.5
1
0.5
0
***
**
n=16
n=10
n=15
n=12
n=12
n=16
WT
fat-3
unc-57
unc-57; fat-3
unc-26
fat-3unc-26
B
Puncta fluor (Fp)
2
1.5
1
0.5
0
n=16
n=10
n=15
n=12
n=12
n=16
WT
fat-3
unc-57
unc-57; fat-3
unc-26
fat-3unc-26

A

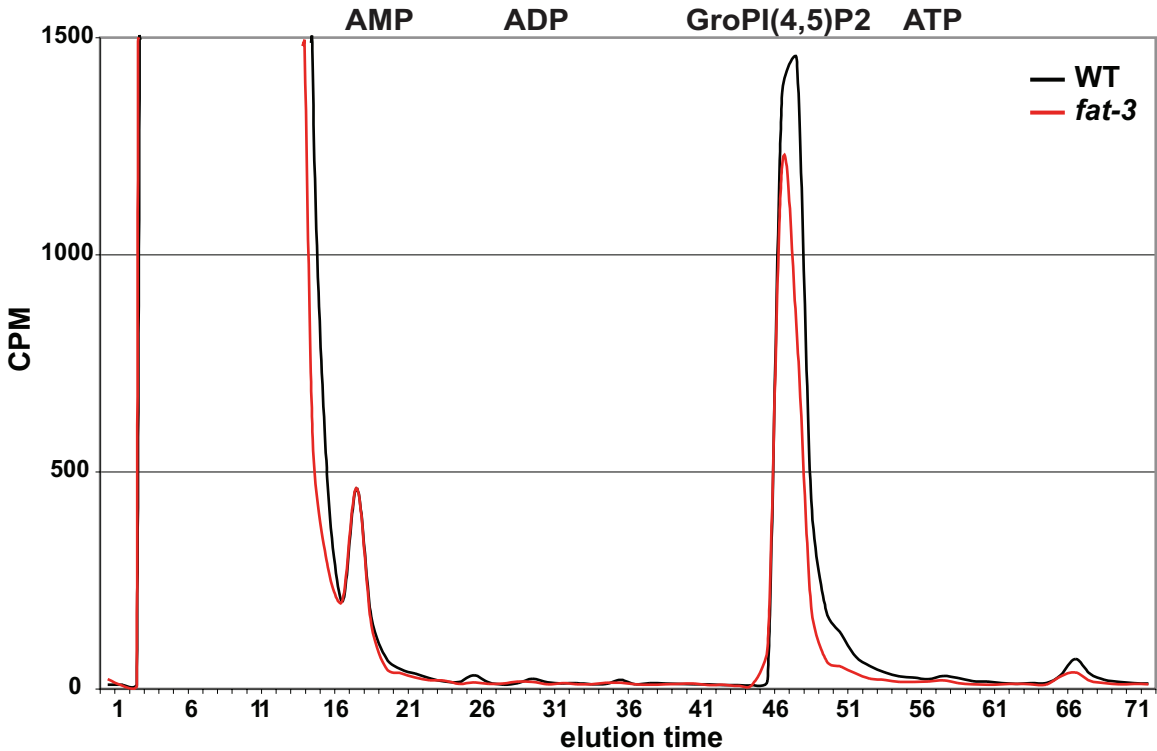
AMP
ADP
GroPI(4,5)P2
ATP
WT
fat-3
1500
1000
500
0
CPM
1
6
11
16
21
26
31
36
41
46
51
56
61
66
71
elution time

B

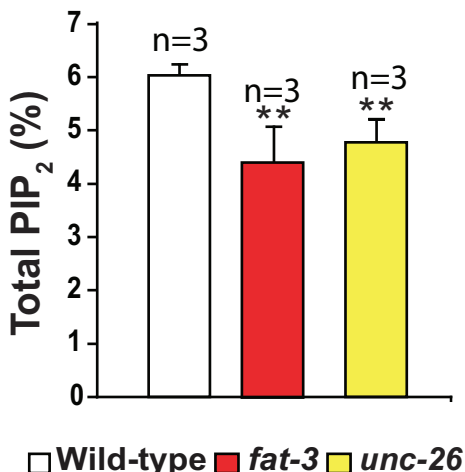
n=3
n=3
**
n=3
**
Total PIP2 (%)
7
6
5
4
3
2
1
0
Wild-type
fat-3
unc-26